

## Multiplane-Stereo PIV measurements for steady flow in the first two bifurcations of the upper human airways during exhalation

Franka Schröder, Michael Klaas, and Wolfgang Schröder

Institute of Aerodynamics and Chair of Fluid Mechanics, RWTH Aachen University  
Wüllnerstr. 5a, 52062, Aachen, Germany, f.schroeder@aia.rwth-aachen.de

### Abstract

To obtain a non-invasive diagnostics for COPD patients it is necessary to understand the flow field in the human lung. The flow within a fully transparent model of the first three generations of a human lung is investigated via multiplane stereo particle-image velocimetry (PIV). The velocity field is recorded in 17 measurement planes within the first two bifurcations of the human lung for ten Reynolds numbers in the range of  $Re_D = 150$  to  $Re_D = 1,150$  during exhalation. The results for 13 parallel measurement planes for three different Reynolds numbers ( $Re_D = 300$ ,  $Re_D = 600$ , and  $Re_D = 1,000$ ) are shown. The measurements in the left subbronchus evidence the development of highly three-dimensional flow structures during steady expiration. Two different vortical structures have been observed for the Reynolds number range. A different influence of the inflow pipes was observed. The superposition of the vortical fluid motion and the upstream fluid transport generates a spiral like flow which leads to a wash-out hypothesis of aerosol particles in the human lung.

**Keywords:** multiplane stereo PIV, human breathing, vortical structures.

### Introduction

Chronic obstructive pulmonary disease, also known as COPD, is a lung disease that usually worsens progressively, is hardly reversible, and can lead to death. Amongst other features, COPD is characterized by airflow obstruction, shortness of breath, and acute exacerbations. Hence, COPD treatment requires an early diagnosis. One possible approach to achieve this goal is to establish a non-invasive diagnostics and clinical monitoring of COPD based on the analysis of exhaled aerosols [1]. Due to the fact that the flow structures during the transition phase between inhalation and exhalation and during exhalation significantly influence the particle deposition of the exhaled aerosols, it is a must to gain detailed knowledge of the temporal and spatial development of these flow structures.

Numerous studies have been carried out to analyze the flow within the human lung. Große et al. [2, 3] analysed the steady and unsteady flow in a realistic model of the first six bifurcations using 2D-2C PIV. On the one hand, they focused on the centerplane of the first bifurcation and analyzed the flow field during steady inspiration and expiration for two different Reynolds numbers. These measurements revealed that the Reynolds number possesses a minor influence on the spatial extension of the flow phenomena as long as it is higher than a critical value that was found to be in the range of  $Re_D = 800 - 1,200$ . On the other hand, they measured the velocity distribution in 13 parallel planes in the first bifurcation during steady inspiration at a Reynolds number of  $Re_D = 1,700$ . They

detected a superposition of the fluid transport in the downstream direction and a pair of counter-rotating vortices to spiral-like shaped vortices. Eitel et al. [4] compared numerical and experimental data for oscillating flow. The experimental investigations were conducted using 2D-2C PIV in the same lung model that has been used by Große et al. [2, 3] for the analysis of the flow in the first bifurcation. The numerical simulations of the flow in the first six generations were based on the Lattice-Boltzmann method. The authors substantiated that the qualitative structure of the complex flow field remains unchanged if a critical mass flux rate is exceeded. Furthermore, the primary flow distribution during expiration, which is more homogeneous in contrast to the inspiration flow distribution and possess higher level of vorticity, is interpreted as a natural particle washout.

To overcome restrictions due to planar datasets and two-dimensional data, Soodt et al. [5] performed stereo scanning particle image velocimetry measurements for the transition from inspiration to expiration in the right main bronchus and the subsequent lobe bronchi for two non-dimensional frequencies, i.e., Womersley numbers ( $\alpha_1 = 3.35$ ,  $\alpha_2 = 4.11$ ), at one peak Reynolds number of  $Re_D = 1,420$ . These measurements showed an increased mass flux into the right superior bronchus for the higher Womersley number, a frequency-dependent phase shift of the flow structures, and a heterogeneous outflow at the beginning of the expiration phase.

These studies evidence the need to investigate the unsteady

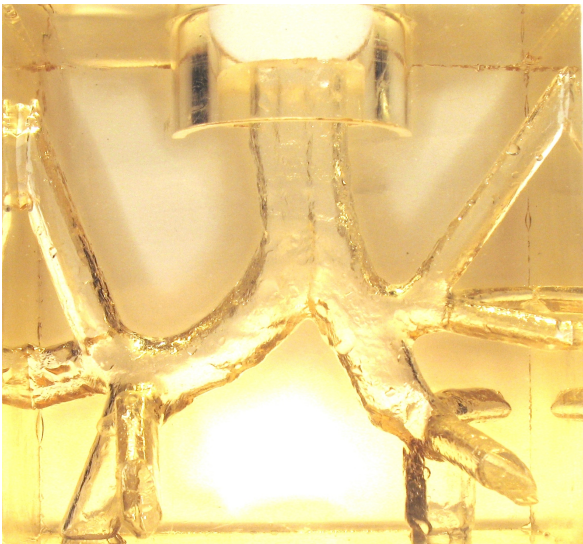


Figure 1 Dorsal view of the lung model.

and three-dimensional flow field in the upper generations of the human lung with high spatial resolution. Hence, the scope of this study is to gain detailed information on the spatial structures of the flow field in the first two bifurcations during exhalation using multiplane stereo PIV. The paper is organized as follows. First, the modeling of the lung flow and the multiplanar-stereo particle-image velocimetry system are described. Second, the results of the PIV measurements are presented and discussed. Finally, these findings are summarized and conclusions are drawn.

## Experimental Facility

### Modeling of the lung flow

The experiments are conducted in a realistic, three-dimensional, transparent lung model (figure 1) that extends to the third generation of the bronchial system. For expiration, the flow enters the lung model through a net of pipes, which have the same diameter as the branches of the third generation of the lung model and that can be considered as straight extensions of these branches. The fluid exits into an anatomically shaped trachea. The hydraulic diameter  $D$  of the trachea is 18.3mm. The measurements at steady expiration have been performed using a closed-circuit flow facility. Since a homogeneous flow circulation has to be guaranteed for an idealized flow distribution in the lung model, the fluid supply for the tank is carefully positioned in the corners of the tank to minimize the fluid influence. Figure 2 shows the experimental setup for steady flow. A water/glycerin mixture with a refractive index of  $n=1.411$  being identical to that of the silicone block of the lung model is used as fluid to ensure optical access without distortion. The optimum mixture for the refractive index of this study's model was found to be 39 mass percent water and 61 mass percent glycerin.

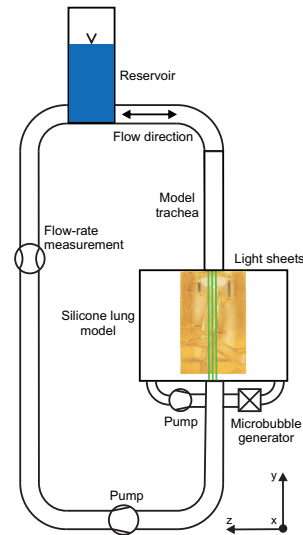


Figure 2 Schematic illustration of the fluid circuit for steady flow.

### Multiplanar-stereo particle-image velocimetry system

All experiments of this study are carried out using the stereo scanning PIV system shown in figure 3. A multipulse Quantel Twins BSL 140 laser operating at a wavelength of  $\lambda = 532 \text{ nm}$  is used as light source. A combination of three lenses (I: convex lens; II: cylindrical lens; III: convex lens) is used to generate the light sheet. The light sheet optics are mounted on a micrometer calliper to guarantee the positioning and movement in 1mm-steps of the lightsheet. Two Photron SA3-120K high-speed cameras are mounted on a Scheimpflug adapter and are synchronized with the laser system by an ILA high-speed synchronizer. The flow is recorded at a sampling frequency of 30 Hz. To guarantee constant path lengths from the object plane to the image plane and as such to keep the image perpendicular to the optical axis, the front walls of the tank have an angle of aperture of  $\alpha = 100^\circ$ .

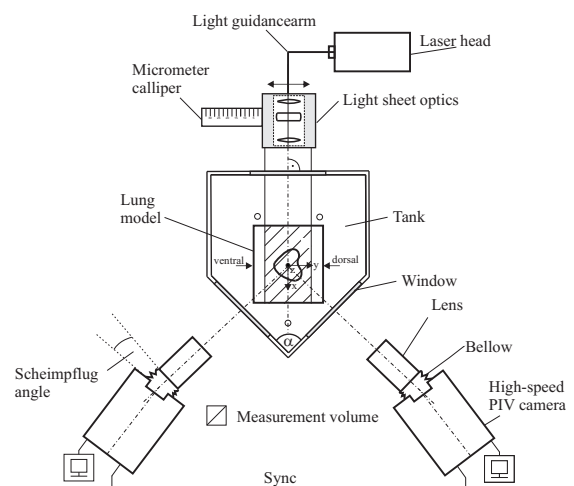


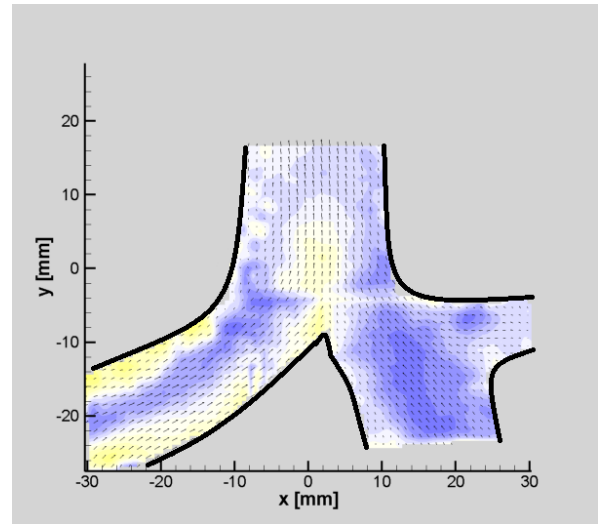
Figure 3 Top view of the optical setup.

Since solid tracers possessed a strong tendency to deposit on the inner surfaces of the model, which led to a considerable decrease in image quality, air-bubbles with a size of 5 to 20 $\mu\text{m}$  generated by a micro-bubble generator with Venturi type mechanism serve as tracer particles. The image post-processing includes decomposing of the images into three parts. A multipass cross-correlation is used to determine the particle displacement and to obtain velocity vectors (VidPIV, Intelligent Laser Applications). The final window size was 32 x 32 pixel with an overlap factor of 50%. This leads to a vector spacing of 0.6mm with 98% of valid vectors. The lateral spacing of the vector field is 1mm and the light sheet thickness is 0.7mm.

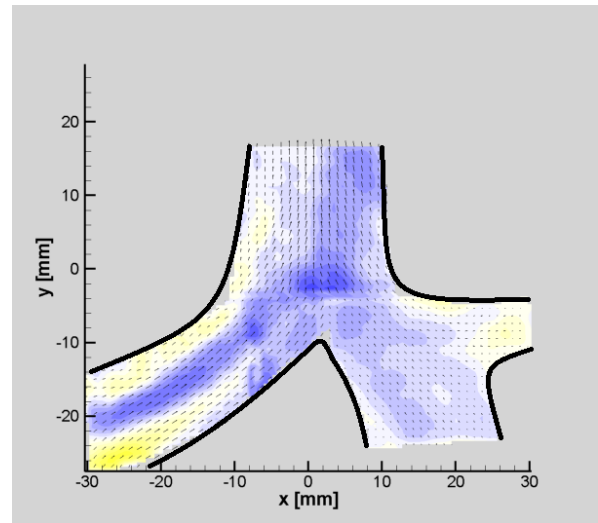
## Results

Figure 4 shows the steady three-dimensional velocity distribution in the center plane of the lung model for all investigated Reynolds numbers ranging from  $Re_D = 150$  to  $Re_D = 1,150$ . The Reynolds number  $Re_D$  is based on the bulk velocity  $U$  and the hydraulic diameter  $D$  determined in the trachea. The vectors in Figure 4 represent the normalized in-plane velocity components  $u/v_{abs}$  and  $v/v_{abs}$ , whereas the colormap represents the magnitude of the normalized out-of-plane velocity component  $w/v_{abs}$  and  $v_{abs}$  is defined as  $v_{abs} = \sqrt{u^2 + v^2 + w^2}$ . The comparison of the velocity distributions in the same measurement plane shows the dependence of the flow structures on the Reynolds number.

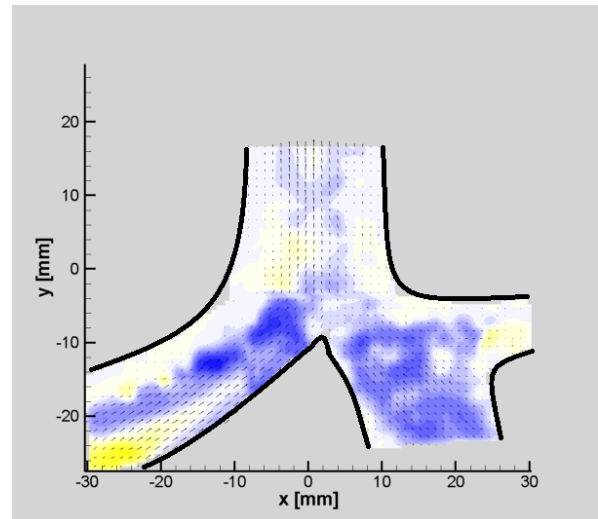
In the right bronchus, the out-of-plane component  $w/v_{abs}$  is negative for all investigated Reynolds numbers. This results from the inclination between the trachea and the bronchus. The colormap and vectors in Figure 4(f) to 4(j) indicate a vortical structure in the upper right lobe bronchus. This flow pattern is generated by the strong curvature of the sub-bronchus. The axis of the vortex vector is almost parallel to the x-y-plane and its spatial extension is on the order of the magnitude of the diameter of the related bronchus.



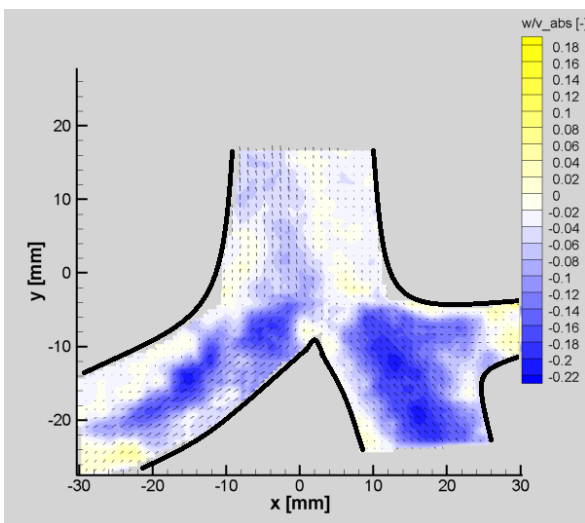
(b)  $Re_D = 300$



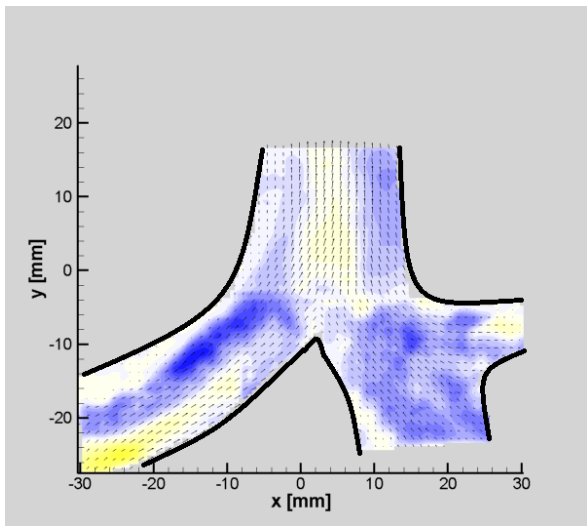
(c)  $Re_D = 450$



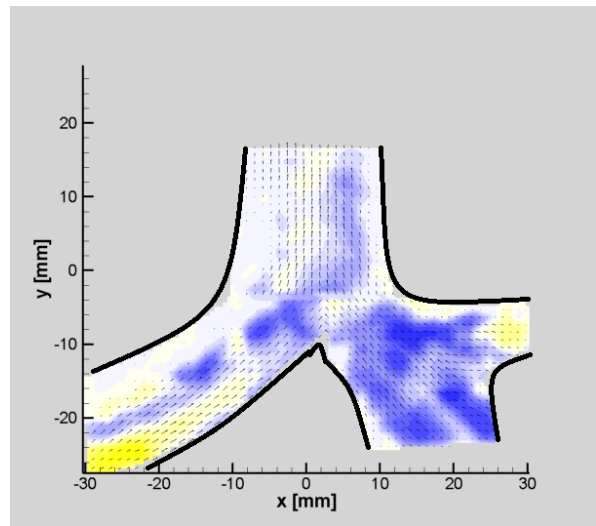
(d)  $Re_D = 600$



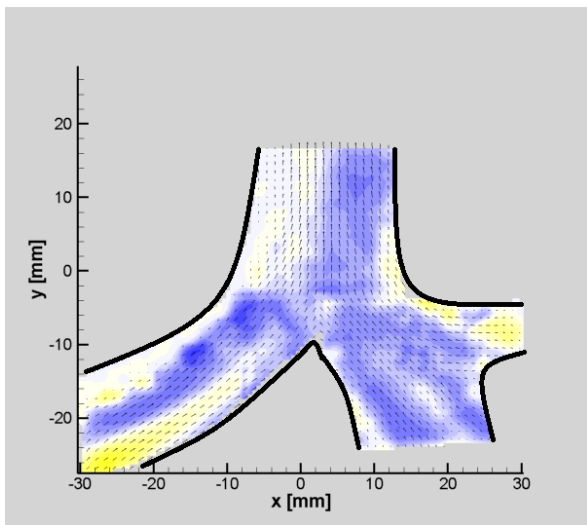
(a)  $Re_D = 150$



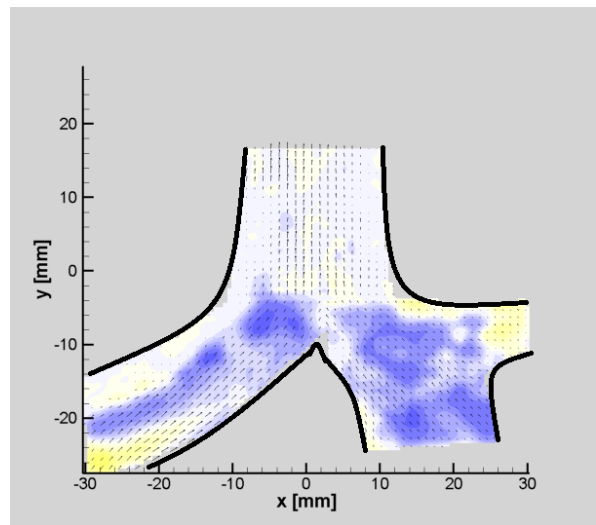
(e)  $Re_D = 700$



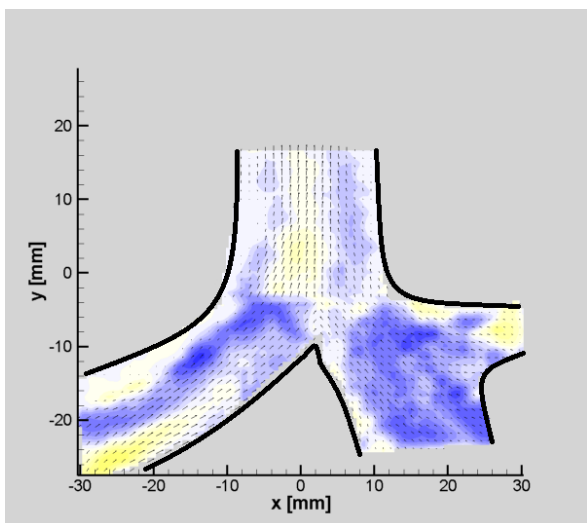
(h)  $Re_D = 1000$



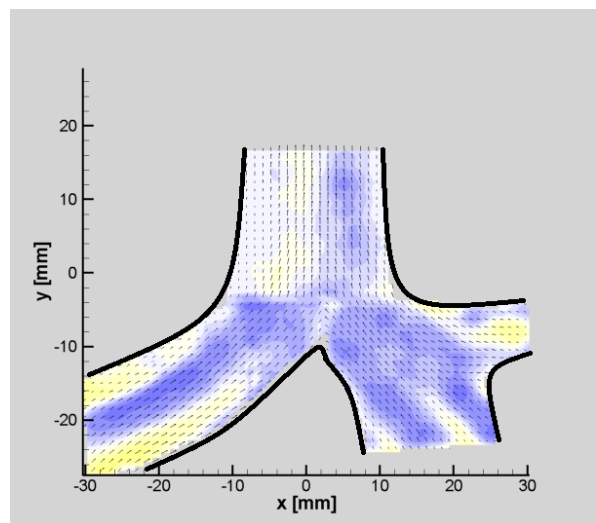
(f)  $Re_D = 800$



(i)  $Re_D = 1100$



(g)  $Re_D = 900$



(j) Reynolds number 1150

**Figure 4** Velocity distribution in the centerplane of the first two bifurcations at 10 Reynolds numbers. The vectors normalized by  $v_{abs}$  indicate the in-plane velocity ( $u, v$ ) and the colormap (see 4(a)) represents the velocity component  $w$ .

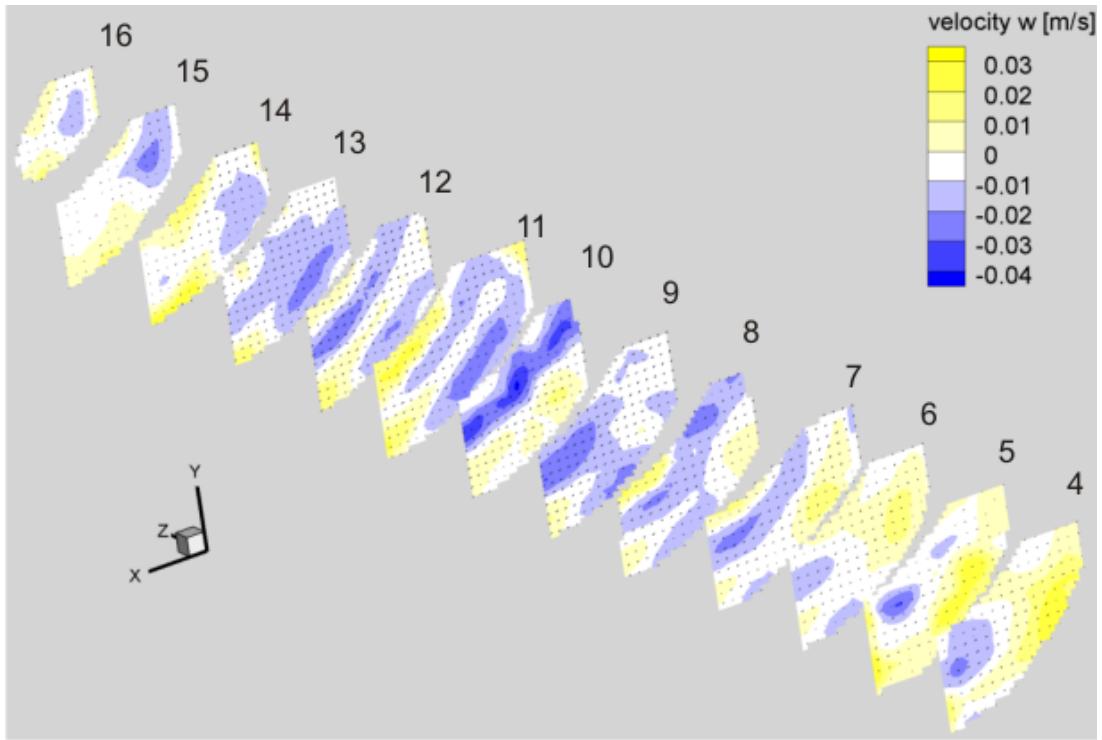


Figure 5 Velocity distribution in 13 measurement planes normal to the z-direction of the left bronchus at  $Re_D = 300$ . The vectors indicate the in-plane velocity  $(u, v)$ , the colormap represents the velocity component  $w$ .

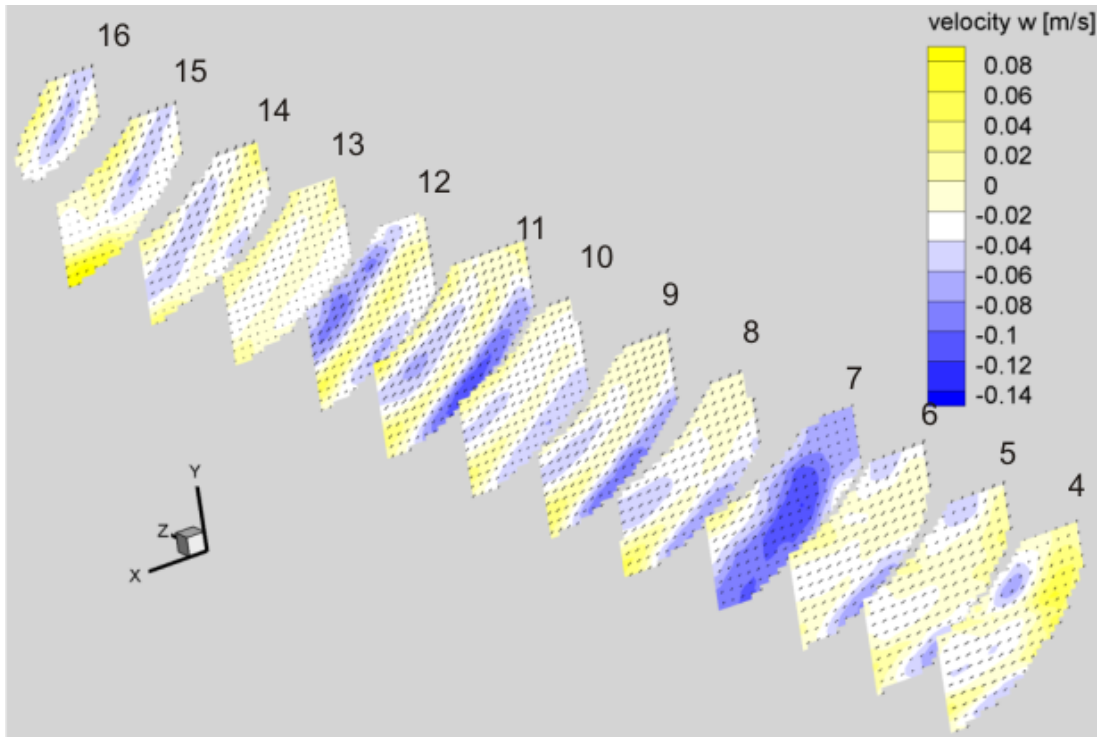
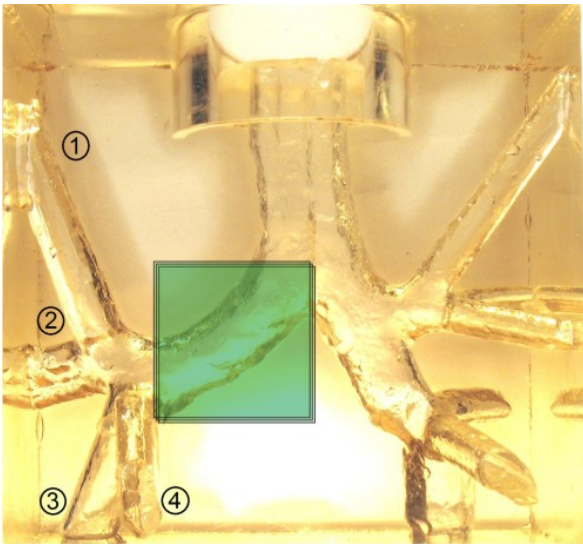


Figure 6 Velocity distribution in 13 measurement planes normal to the z-direction of the left bronchus at  $Re_D = 600$ . The vectors indicate the in-plane velocity  $(u, v)$ , the colormap represents the velocity component  $w$ .



**Figure 8 Dorsal view of the lung model**

In the left bronchus the out-of-plane component reaches its maximum near the inner wall. In the center of this bronchus a corresponding negative component can be seen. To better understand of the three-dimensional flow structure in the left lobe bronchus figures 5 to 7 show 13 planes normal to the  $z$ -direction for  $Re_D = 300$ ,  $Re_D = 1000$ , and  $Re_D = 1,150$ , respectively. The images show the three-dimensional velocity distribution with the vectors indicating the in-plane velocity components  $u$  and  $v$  and the colormap representing the out-of-plane component  $w$  of the velocity field. The in-plane and out-of-plane velocity distribution in the measurement planes are the mean of 400 measurements. Their composition yields the three-dimensional extension of the vortices.

For  $Re_D = 300$  various flow structures can be identified. In the planes 11 and 12 two vortices can be observed. The first vortex center is in the measurement plane 12. This vortex is located at the outer wall and rotates counter clockwise. The center of the second vortex, also rotating counter clockwise, is located in the measurement plane 11 at the inner wall. Both vortices are caused by the inflow from the upstream branch of this bifurcation generation which is denoted by ① in figure 8 and which forms a u-shaped pipe with the left lobe bronchus and the second upper inlet pipe (②). Similar to the aforementioned vortices, one further spiral-like structure can be observed in the measurement planes 7 and 8 which results from the inflow from the two lower branches (③) and (④).

The analysis of the flow field in the left bronchus for a Reynolds number of  $Re_D = 600$  in figure 6 shows that the counter clockwise rotating vortices in the measurement planes 11 and 12 are also present for the higher Reynolds number. In contrast to the findings for  $Re_D = 300$ , a high negative out-of-plane velocity can be observed in the measurement plane 7. In conjunction with the high positive out-of-plane velocity in the measurement planes 4 and 5, the results indicate that the vortex strength as well as the vortex size and thus the mass flux from the lower branches

increases at large Reynolds numbers.

For  $Re_D = 1000$ , a pair of counter-rotating vortices can be observed in the measurement planes 9 to 15 with the centers in the measurement planes 11 and 12. The spatial dimension of those vortices is significantly higher than that of the two counter clockwise rotating vortices at  $Re_D = 300$  and  $Re_D = 600$ .

The flow in the bronchus and inlet pipe ① can be compared with the flow field in an u-shaped pipe. Humphrey et al. [7] simulated the flow through a u-shaped pipe and compared the numerical results with experimental data from Agrawal et al. [8]. To characterize the flow in this region the Dean number  $De = Re \cdot \sqrt{D/2R}$  is used where  $R$  is the radius of the curvature and  $D$  the hydraulic diameter. Humphrey et al. [7] showed that at increasing Dean number different secondary flow patterns establish. They detected two critical Dean numbers for the development of four counter-rotating vortices. The first pair of vortices appears at a Dean number of  $De \approx 180$  and the second at  $De \approx 560$ .

In the case of the human lung the flow field for a Reynolds number  $Re_D = 1,000$  shows two counter-rotating vortices. For this bronchus a Dean number of  $De = 500$  at a local Reynolds number of  $Re = 800$  results. This Dean number is in the range where a pair of vortices appears. At lower Reynolds number there exists two counter-clockwise rotating vortical structures influenced by the variation of the pipe, i.e., the curvature changes in the streamwise direction and the geometry is perturbed by the additional endings on the outer circumference of the model  $90^\circ$  of the u-shaped pipe.

The former observations lead to the conclusion that the sense of rotation, the size, and the strength of the vortical structures that develop during exhalation depend significantly on the Reynolds number and hence on the phase of breathing cycle. Second, the vortical fluid motion is determined by the interaction of a pipe-bend-like flow with a jet-like from the higher branches. Third, these results lead to the hypothesis that the human lung might offer a natural wash-out process in specific regions. The particles produced in the lower human airways due to a re-opening of a collapsed terminal airways are convected by the airflow even through complicated geometric regions and the described vortical structures prevent the deposition of the particles at the wall of the lung.

## Conclusions and Outlook

Multiplane stereo PIV measurements have been carried out in several parallel planes within the first two bifurcations of a model of the human lung. Three-dimensional velocity fields for 10 Reynolds numbers have been presented. The velocity fields show the flow within the lung model to possess a highly three-dimensional character. The flow in the trachea is strongly influenced by the inlet velocity from the subbranches. The flow field in the left bronchus is strongly influenced by the Reynolds number and different out-of-plane phenomena have been observed. The details have been analyzed for  $Re_D = 300$ ,  $Re_D = 600$ , and

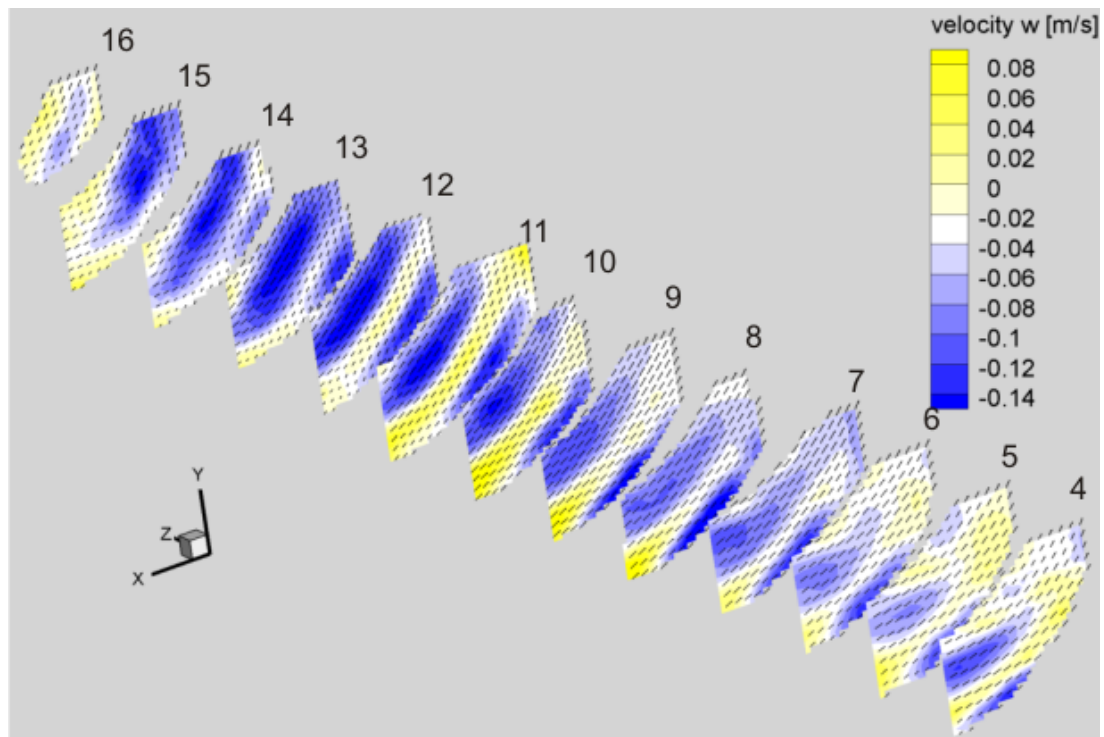


**Figure 7** Velocity distribution in 13 measurement planes normal to the z-direction of the left bronchus at  $Re_D = 1000$ . The vectors indicate the in-plane velocity  $(u, v)$ , the colormap represents the velocity component  $w$ .

$Re_D = 1,000$  in 13 parallel planes. Two different vortical structures have been observed. For  $Re_D = 300$  and  $Re_D = 600$  two counter-clockwise rotating vortices were found. For a Reynolds number of  $Re_D = 1,000$  a pair of counter-rotating vortices that is well-known from pipe-bend flows was detected. Since spiral-like flow phenomena have been identified which ensure a natural wash-out process particles produced in the lower airways are able to follow the contour and the vortical structure avoid a deposition. Due to this fact the particles can be exhaled and their deposition can be analyzed which could lead to a non-invasive diagnostics and clinical monitoring of COPD based on the analysis of the exhaled aerosols.

Further research will include the investigation of the flow field in those planes for a six generation lung model to verify, if the hypothesis independent from the inflow conditions.

### Acknowledgements

The funding of the 'Deutsche Forschungsgemeinschaft' in the frame of the joint program "'EXHALAT'" is gratefully acknowledged.

### References

- [1] Haslbeck, K., Schwarz, K., Hohlfeld, J. M., Seume, J. R. & W. Koch (2010) Submicron droplet formation in the human lung. *J Aerosol Sci*, **41**, 429–438.
- [2] Große, S., Schröder, W., Klaas, M., Klöckner, A. & Roggenkamp, J. (2007) Time Resolved Analysis of Steady and Oscillating Flow in the Upper Human Airways, *Exp. Fluids*, **42(6)**, 955–970.
- [3] Große, S., Schröder, W., Klaas, M., Klöckner, A. &

- Roggenkamp, J. (2008) Time-resolved PIV measurements of vortical structures in the upper human airways. *Topics of applied physics: Particle image velocimetry - new developments and recent applications*, editors A. Schröder and C. Willert, Springer, 35-53.
- [4] Eitel, G., Soodt, T. & Schröder, W. (2010) Investigation of pulsatile flow in the upper human airways *Int J Des Nat Ecodyn*, **5(4)**, 335–353.
- [5] Soodt, T., Schröder, F., van Overbrüggen, T., Klaas, M., Schröder, W. (2011) Experimental investigation into the transitional bronchial velocity distribution using stereoscanning PIV *Exp Fluids*, DOI: 10.1007/S00348-011-1103-5.
- [6] Graftieaux, L., Michard, M., Grosjean, N. (2001) Combining PIV, POD and vortex identification algorithms for the study of unsteady turbulent swirling flows. *Meas Sci Technol*, **12**, 1422-1429.
- [7] Humphrey, J.A.C., Iacovides, H., Launder, B.E. (1985) Some numerical experiments on developing laminar flow in circular-sectioned bends *J. Fluid Mech.*, **154**, 357-375.
- [8] Agrawal, Y., Talbot, L., Gong, K. (1978) Laser anemometer study of flow development in curved circular pipes *J. Fluid Mech.*, **85**, 497-518.